Point-defect energies in the nitrides of aluminum, gallium, and indium

T. L. Tansley and R. J. Egan
Semiconductor Science and Technology Laboratories, Physics Department, Macquarie University, New South Wales 2109, Australia
(Received 28 June 1991)

Experimental data on the nature and energetic location of levels associated with native point defects in the group-III metal nitrides are critically reviewed and compared with theoretical estimates. All three show strong evidence of the existence of a triplet of donorlike states associated with the nitrogen vacancy. Ground states are at about 150, 400, and 900 meV from the conduction-band edge in InN, GaN, and AlN, respectively, with their charged derivatives lying closer to the band edge. These values agree with both modified-hydrogenic and deep-level calculations, surprisingly well in view of the inherent approximations in each in this depth range. The InN donor ground state is both optically active and usually occupied, showing a distinctive absorption band which is very well described by quantum-defect analysis. Variation of threshold with electron concentration shows a Moss-Burstein shift commensurate with that observed in band-to-band absorption. In both GaN and AlN, levels have been identified at about $\frac{1}{4}E_G$ and about $\frac{3}{4}E_G$, which correlate well with predictions for the antisite defects N_M and M_N, respectively, while similar behavior in InN is at odds with theory. The metal-vacancy defect appears to generate a level somewhat below midgap in AlN and close to the valence-band edge in GaN, but has not been located experimentally in InN, where it is predicted to lie very close to the valence-band edge. A tentative scheme for the participation of two of the native defects in GaN, namely V_N and N_{Ga}, in the four broad emission bands found in Zn-compensated and undoped GaN is offered.

I. INTRODUCTION

The nitrides of the three group-III metals Al, Ga, and In have received attention varying between the sporadic and the sustained, as specific applications have been promoted, and as a sequence of material growth and processing strategies have emerged.

Indium nitride is an n-type semiconductor with a band gap in pure material of 1.9 eV,[1] often Moss-Burstein shifted to about 2.05 eV in the more commonly produced samples of high electron concentration.[2–6] The low conduction-band density of states responsible for this shift suggests that the conduction electron is light and its mobility therefore high, an inference substantiated in experimental values[7] as high as 4×10^3 cm^2 V^{-1} s^{-1} in relatively poor polycrystalline samples of $n\sim10^{17}$ cm^{-3}. This combination of wide gap and high electron mobility suggests that useful devices, including those luminescent in the orange spectral region, can be constructed eventually, although we are unaware of any reports of efficient photon emission or of successful counterdoping of this compound.

The blue electroluminescence characteristic of gallium nitride has been of interest over a number of years,[8–13] revived more recently as viable vapor phase epitaxial (VPE) growth methods have been developed.[14,15] Although direct band-to-band recombination delivers an ultraviolet (365 nm) photon of 3.39 eV, broadband emission is found over much of the visible spectrum[16] depending upon a combination of extrinsic influences including choice of dopant and growth method. As-grown material may be semi-insulating or n type, although doping with magnesium is reported[17,18] to produce genuinely p-type material.

Aluminum nitride, in common with the gallium compound, has attracted interest as a result of both insulating and piezoelectric properties.[19] The band gap is 5.9 eV, although this may be reduced by a few percent if stoichiometry is not maintained, or increased by a similar margin when oxygen is present as the oxynitride.[20] AlN has excellent insulating properties, low dielectric loss, and dispersion of permittivity,[21] and can be prepared at low temperature on GaAs substrates[22] leading to the possibility of metal-insulator-semiconductor (MIS) structures entirely within the III-V system.[23–25]

Each of these potential applications requires, among other factors, an understanding of the nature of native defects in each material and in particular the charge states and energies of electron levels generated by the four residual points defects (metal vacancy V_M, nitrogen vacancy V_N, and antisite defects M_N and N_M) likely to persist even under optimal growth conditions. Such states may trap carriers, either presenting a space charge particularly undesirable in MIS structures or increasing the density of point charges with a consequent degradation of mobility in conductive material. Deep levels, particularly these close to midgap, offer preferential recombination routes, frequently nonradiative and thus inimical to luminescent devices. Since autocompensation, involving the interaction between dopant atoms and doping-generated point-defect compensators, has purportedly limited the range of applications of direct wide-gap II-VI compound semiconductors, it is possible that similar interactions may be influential in the M^{III}-N system. It is therefore germane to examine the substantial amount of experimental evidence for the existence and nature of point-defect levels in these compounds, in the light of theoretical guidance provided by Jenkins and Dow.[26]

Since calculated electronic structures show the same commonalty of features across all three compounds as do a broader range of properties,[27] we remark first, on general theoretical and experimental approaches.

II. THEORETICAL CONSIDERATIONS

The predictions of energy levels of either intrinsic defects or extrinsic impurities in III-V semiconductors is fraught with the difficulty of balancing the contributions of core effects at short range and the more extensive Coulomb effects. In general, one approach alone is employed and the other either neglected in a first approximation or included as a refinement *a posteriori*. Here we summarize methods appropriate to intrinsic defects in the group-III metal nitrides (M^{III}-N).

A. Hydrogenic centers

Where the potential surrounding the defect varies only slowly, an effective mass treatment can be employed. This is appropriate when the amount of electronic charge remaining in the region of the short-range potential is sufficiently small for the conditions imposed by the character of the solution in that region to be minor. Since the electron or hole moves in a long-range potential analogous to that of a hydrogen atom the appropriate centers, shallow donors or acceptors are treated as "hydrogenic." The energy levels are given in terms of the effective Rydberg energy $\mathcal{R}^*_{\mathrm{H}}$ by

$$E=\mathcal{R}^*_{\mathrm{H}}/n^2 \quad \text{where } \mathcal{R}^*_H=q^2m^*/2(4\pi\epsilon_r)^2\hbar^2 . \tag{1}$$

This result is valid only for shallow, single donors or acceptors in nonpolar semiconductors with spherical constant energy surfaces close to the band extrema. Only the last of these conditions is met in M^{III}-N compounds and only the nitrogen vacancy V_{N} is sufficiently shallow in all three to be susceptible to a hydrogenic treatment.

Substituting Zq for q for a multiple donor of degeneracy Z extends the model successfully to excited states while underestimating the ground-state energy.[28]

Extension to polar materials requires the inclusion of the coupling between electron and optical phonon modes. The collective, polaron, excitation has mass m_p^* given, in the usual nomenclature, by

$$m_p^*=(1+\alpha/12)/(1-\alpha/12) ,$$
$$\text{where } \alpha=(q^2/4\pi\epsilon_0 h)(\epsilon_\infty^{-1}-\epsilon_s^{-1})/(m^*/2\hbar\omega)^{1/2} . \tag{2}$$

Here ϵ_∞ and ϵ_s are the high- and low-frequency relative permittivities, respectively.

Table I brings together calculated hydrogenic ground and first excited energies for hydrogenic donors in the M^{III}-N compounds and relevant parameters. Equivalent data for GaAs and InP are included for comparison. The correct choice of a value for permitivity, ϵ_r, in Eq. (1) is made, following Ridley,[28] by observing that $R^*_{\mathrm{H20}} > h\omega_{\mathrm{TO}}$ for all three nitrides so that $\epsilon_r=\epsilon_\infty$.

The photoionization process which takes an electron from a neutral hydrogenic donor into a parabolic conduction band is characterized by an absorption coefficient α_{H} which depends on photon energy $\hbar\omega$ as

$$a_{\mathrm{H}} \propto (\hbar\omega-E_D)/(\hbar\omega)^5 \tag{3}$$

where E_D is the excitation threshold energy.

Equation (3) represents a narrow absorption peak whose maximum is at an energy $5E_D/4$. In a typical experiment, the threshold is much more sensitive than the peak to thermal broadening, so the latter is used to estimate the former.

In most semiconductors the mobility of a thermally generated free electron is sufficiently insensitive to temperature to allow a direct interpretation of donor depth from temperature dependence of conductivity $\sigma(T)$, since

$$\sigma(T)=\sigma_0\exp(-E_D/kT) . \tag{4}$$

The value of E_D obtained experimentally from Eqs. (3) and (4) may not coincide since the techniques do not measure the same quantity. While the optical measurement defines the energy of the donor in the equilibrium lattice configuration for the occupied state, the thermal measurement gives an average over the ensemble of occupied and unoccupied states. There may be a significant difference in the strongly polar lattices of the nitrides, for which available experimental data are discussed in Sec. III.

B. Quantum defects and deep levels

Even if core effects cannot be ignored, an effective mass approach may still be appropriate provided a quantum-defect ground-state wave function is used. Here the absorption coefficient α_Q for a neutral center, a deeper occupied donor, for example, becomes

$$\alpha_Q \propto (\hbar\omega-E_Q)^{3/2}/(\hbar\omega)^3 . \tag{5}$$

A significant feature of this result is that the energy at the absorption peak is twice that at the threshold E_Q.

TABLE I. Data for modified-hydrogenic calculations. All energies are in meV. Suffixes to Rydberg constants $\mathcal{R}^*_{\mathrm{H}}$ are 1 and 2, singly and multiply charged donor states; *O* and *P*, unmodified and polaron-modified values.

	ϵ_∞	ϵ_s	m^*/m	$\hbar\omega_{\mathrm{LO}}$	$\hbar\omega_{\mathrm{TO}}$	$\mathcal{R}^*_{\mathrm{H10}}$	$\mathcal{R}^*_{\mathrm{H20}}$	$\mathcal{R}^*_{\mathrm{H1}P}$	$\mathcal{R}^*_{\mathrm{H2}P}$	α	m^*_{p01}
InN	8.4	15.3	0.12	89	57	23	90	24	94	0.24	1.04
GaN	5.5	10	0.20	79	70	90	360	97	390	0.48	1.083
AlN	4.7	8.5	0.33	97	82	200	800	216	890	0.65	1.114
GaAs	10.9	13.18	0.067	30	32	5.24		5.33		0.088	1.015
InP	9.5	12.35	0.08	39	43	7.14		7.29		0.127	1.021

Ridley defines the quantum defect[28] as $D=|v_T-1|$, in terms of the ratio of the hydrogenic-calculated depth to experimental threshold $v_T=(\mathcal{R}_H^*/E_T)^{1/2}$, where E_T is the measured threshold. When D is close to zero a hydrogenic treatment would appear appropriate while large values would indicate the need for a proper deep-level analysis. If D is of order unity, however, Eq. (5) should describe the observed absorption features.

The energies associated with deep levels, where the effective mass approximation breaks down completely, can be determined using techniques not unlike band-structure calculations. Jenkins and Dow[26] and others[29,30] have employed a technique attributed to Hjalmarson *et al.*[31] in which deep impurity levels are obtained by solving the Schrödinger equation $H|\phi\rangle=E|\phi\rangle$. Here $H=H_0+V$, H_0 is the Hamiltonian for the host crystal and V is an effective defect potential, centered at the site of the defect and defined over an effective radius a^*, within which it is strong, given by $a^*=(\hbar^2/m)/(q^2/4\pi\epsilon_0)$.

Empirical tight-binding theory is used to determine V, but the effects of long-range Coulombic potentials and charge splittings of the levels are neglected. It is said that uncertainties of a few tenths of an eV result,[26] clearly of experimental significance in the case of levels in the proximity of the band edges.

Cross sections for the photoionization of deep levels depend upon whether the impurity state is $|s\rangle$-like or $|p\rangle$-like. The relevant absorption coefficients take the form

$$\alpha_{DS}\propto(\hbar\omega-E_{DS})^{3/2}/\hbar\omega \quad (|s\rangle)\,, \tag{6a}$$

$$\alpha_{DS}\propto(\hbar\omega-E_{DP})^{1/2}/\hbar\omega \quad (|p\rangle)\,. \tag{6b}$$

Since (a) deep-level threshold energies are large, by definition, and (b) densities of states away from the band extrema cease to be parabolic, the likely range of usefulness of (6) is confined to the vicinity of the experimental absorption edge.

C. Real materials

Much of the experimental work reported on the nitrides has involved polycrystalline thin films with large surface area to volume ratios in which surface states play an important role. Single-crystal GaN and AlN have been studied but not specifically for defect properties. Recent advances in deposition of GaN films,[15,18] in particular by molecular beam epitaxy (MBE) and metalorganic chemical vapor deposition (MOCVD), may permit the resolution of some of the unresolved features of defect behavior.

Each of the nitrides is also susceptible to oxygen contamination on exposure to atmosphere. In the case of InN a few surface monolayers are converted to the oxide[32] while absorption bands at 4.45 and 4.95 eV in AlN have been ascribed to oxygen.[33] The problems are most acute in AlN where an oxygen solubility limit of 8% is reported[34] and both the oxide and oxynitride may occur during growth unless strict precautions are taken for the exclusion of the impurity from both deposition system and precursors.[20,22]

III. EXPERIMENTAL DATA

In comparison with other III-V compounds, basic data on the optical and electronic properties of InN and AlN are sparse while GaN has been more widely studied. In the following discussion of experimental results, data are quoted for material prepared by a variety of techniques, often with little detail reported on either the method or the micromorphology of the product. Since these are crucial to the determination of defect content, it is not possible to speculate in most cases whether the defects ascribed to particular energy levels are plausible. Our previously published results[1,7,27] have all been obtained on radio frequency reactively sputtered (RFRS), polycrystalline films. Results appearing here are from films grown by either RFRS or laser activated chemical vapor deposition (LCVD).[22]

A survey of the room-temperature optical-absorption spectra of InN, GaN, and AlN in the energy range 40 meV–6 eV shows the three compounds to have a number of features in common: (a) direct band-to-band absorption edges, (b) band-edge tails and midgap absorption features of extrinsic origin and associated with crystal defects, and (c) optical phonon absorption structure in the infrared. Each of the compounds additionally shows at least one electron trap capable of thermal excitation into the conduction band over some temperature range.

Band-to-band absorption in polycrystalline RFRS film samples is shown in Fig. 1 where the square dependence of absorption coefficient on photon energy is typical of direct Γ (Γ_0^v-Γ_1^c in this case) transitions and yields minimum transition energies of 1.94, 3.40, and 5.94 eV for InN, GaN, and AlN, respectively. The value for InN, which shows a significant Moss-Burstein shift above the low electron concentration limit of 1.89 eV, is for a sample of $n\approx10^{19}$ cm^{-3}. We now discuss the levels introduced by the native defects in each of the nitrides. The depth of all levels is described with respect to the bottom of the conduction band as this is how they are observed experimentally.

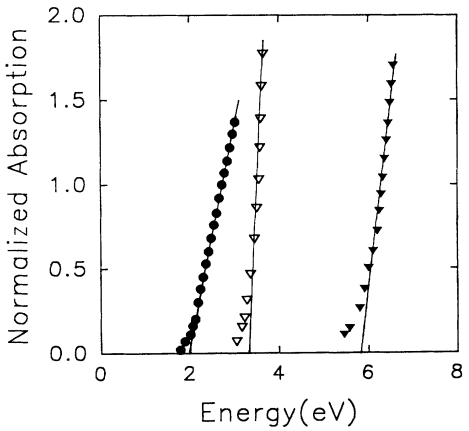

FIG. 1. Direct band-to-band absorption edges of InN, GaN, and AlN films obtained by radio-frequency reactive sputtering (adapted from Ref. 27).

A. Gallium nitride

GaN, with a band gap of 3.4 eV (Fig. 1) has proven to be rather easier to prepare than the other nitrides and a good deal of information on defect levels has been gathered. This is collected with relevant calculated values in Fig. 2. Shallow donor levels have been reported in GaN with energies 10–40 meV (Refs. 37–40) (group A) and 110–115 meV (Refs. 38, 40, and 41) (group B) both from the temperature dependence of carrier concentration and optically. Single reports of miscellaneous energy levels in this region also exist although, in general, their nature has not been posited. Vavilov *et al.*[42] suggest either impurities or native defects to be responsible for the 110-meV level, considering also the possibility of absorption by excitons although these are now known to be considerably shallower. Tansley, Egan, and Horrigan[27] invoked nitrogen vacancies although their RFRS GaN was consistently insulating, with the Fermi level sufficiently far removed from the conduction-band edge for neither thermal nor optical stimulation of shallow levels to be possible. Thermal activation analysis of insulating GaN reveals a deeper donor (group C of Fig. 2), the depth of which varies from sample to sample; examples at the extremes of our range at 0.3 and 0.46 eV are shown in Fig. 3. A range of values between 0.23 (Ref. 40) and 0.39 eV (Ref. 41) have been reported elsewhere and generally coincide with a modified-hydrogenic estimate of about 0.39 eV (Table I). We therefore suggest that the three electron states associated with V_N in GaN are located at about 30 meV, 100 meV, and 0.4 eV below the conduction band, none therefore being resonant with it.

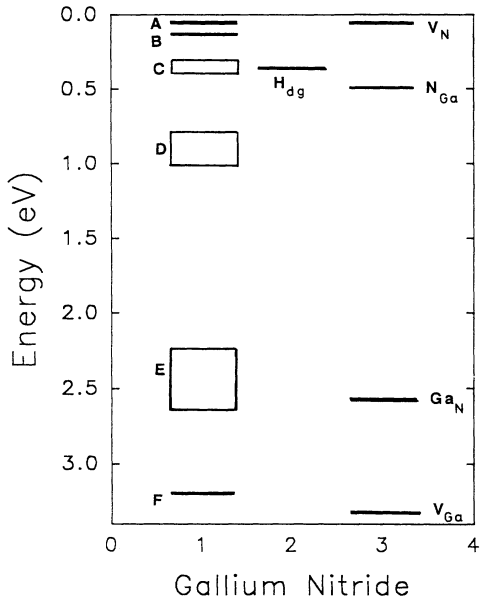

FIG. 2. Distribution of defect levels in the band gap of GaN. The states in column 1 are those reported from experimental studies and fall into six groups A–F. The gallium vacancy, F, at E_G-3.264 eV is often seen in luminescence studies. Column 2 shows the result of donor-level calculations in the modified-hydrogenic approximation from Table I. Column 3 data are the electron states for the point defects indicated, as calculated in Ref. 26.

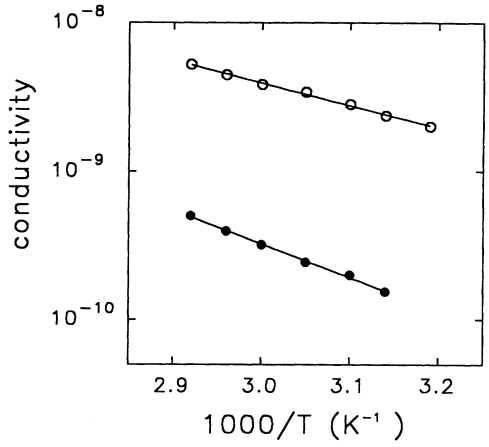

FIG. 3. Two examples of thermally activated conductivity in insulating GaN films prepared by RFRS. Activation energies are 305 meV (○) and 460 meV (●).

A deep level is observed in thermal activation to be between 0.8 and 1.1 eV below the conduction-band edge[41,43] (group D of Fig. 2) and has been variously attributed to gallium vacancies or carbon impurities. A better interpretation is that the level represents the nitrogen antisite defect predicted by Jenkins and Dow.

The deep trap (group E of Fig. 2) which we observe as a band-tail absorption feature[27] has a threshold in the range 2.3–2.7 eV when plotted as an $|s\rangle$-like level. An example is included in Fig. 4 along with similar levels in InN and GaN. The proximity of the level to the 2.8-eV prediction for Ga_N of Jenkins and Dow suggests a correspondence.

A level at 3.264 eV (F) has been positively identified[12,44,45] (by photoluminescence of doped single-crystal GaN) to be a result of gallium vacancies and agrees well with the location predicted by Jenkins and Dow.

Much of the detail available from luminescence spectroscopy of GaN is concerned with samples including at least one of (i) heavy doping, (ii) high compensation lev-

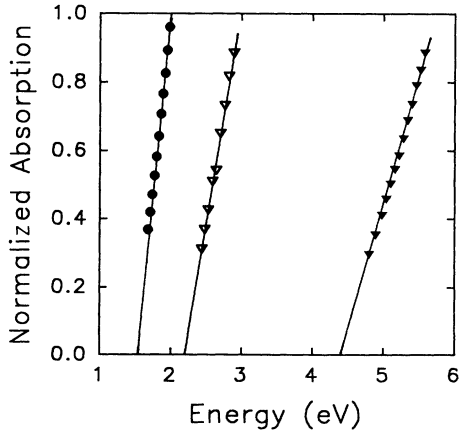

FIG. 4. Absorption data for deep levels in InN (●), GaN (▽), and AlN (▼). In accordance with Eq. (6a), the absorption coefficient α is plotted as $\alpha^{2/3}(\hbar\omega)$ versus $\hbar\omega$ and yields threshold energies of about $\frac{2}{3}E_G$ in each case.

els, and (iii) nonideal crystallinity. It is clear from a survey of the published data that many spectral features are independent of the introduced species and therefore involve native defects.

Edge emission at room temperature and in undoped material is at 365 nm (3.39 eV), an excitonic photoluminescence peak displaced by about 30 meV from the direct band-to-band transition energy. Study of this feature at lower temperature has furnished much detail on exciton structure in GaN.[42,46]

The introduction of zinc as a compensating center generates a broad blue emission peak centered at about 2.92 eV,[47] indicating a recombination center at about 470 meV above the valence band. Extinction of this peak at higher temperatures has a dependence suggesting a relaxation energy of about 330 meV for this center acting as a hole trap in thermal exhaustion. Coincidentally, the introduction of phosphorus as an alternative compensator to zinc yields almost identical photon and hole emission energies.[48]

In addition to the blue peak, GaN:Zn emits broad bands in the green (centered at about 2.6 eV), orange-yellow (2.2 eV), and red (1.8 eV) regions.[16,49] While the 2.6-eV band requires Zn (or other similar) compensation, the 2.2-eV emission occurs in VPE grown material in which carbon has precipitated.[50] Most significantly, this band has been observed in samples implanted with no less than 35 atomic species,[51] clear evidence of its defect-related nature. The red emission band is variously reported as centered between 1.65 and 1.85 eV, is also certainly defect-related, but appears to have some dependence upon the impurity species introduced.[51]

A possible scheme for the involvement of the defects identified in Fig. 2, and in view of the above discussion, is suggested in Fig. 5. Band-to-band emission at 3.39 eV (transition I) is superseded by preferential recombination via the compensator when zinc is introduced (II), yielding blue 2.92-eV luminescence and locating the zinc level at about E_V+470 meV. Since the nonstoichiometric nitrogen vacancy is always likely to be present, donor-acceptor recombination is an obvious candidate for green emission (III). A peak centered at 2.56 eV would require V_N to be located about 360 meV below the conduction band and this correlates well with both calculated and measured values for donor ground-state energy.

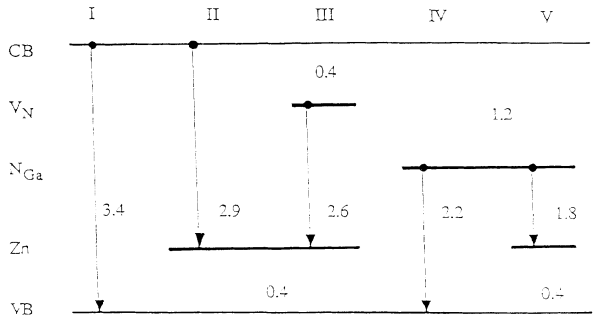

FIG. 5. Suggested scheme for the involvement of native defects in the four principal luminescence bands (II: blue, III: green, IV: orange-yellow, V: red) in GaN, either Zn compensated or undoped. The ultraviolet emission (I) is direct band-to-band recombination emission.

The independence of orange-yellow emission (IV) of extrinsic dopants suggests the participation of a defect level at a depth of about 1 eV and the experimentally observed center, which we have suggested is associated with the N_{Ga} antisite defect (Fig. 2), is an obvious candidate. Finally, we point out that the energy difference between this center and those induced by a group of impurities, including P and Zn is about 1.75 eV. The location of this energy within the red emission band leads us to the tentative allocation (V) of red emission to a N_{Ga}-acceptor transition.

B. Indium nitride

InN has received very little attention because of the difficulty inherent in the preparation of stoichiometric samples. High mobility material with electron concentrations below 10^{17} cm^{-3} at room temperature has been prepared by RFRS with balanced target nitridation.[35] Figure 6 identifies the five distinguishable energy levels observed in the gap and further includes the results of the hydrogenic calculations from Table I and the deep-level calculations of Jenkins and Dow.

1. Shallow levels

A shallow level appears as a shoulder at 50 meV on the 60-meV infrared absorption peak associated with the LO phonon.[27] The associated threshold energy of 40 meV agrees well with the 45–50-meV thermal activation energy measured in samples with carrier concentration be-

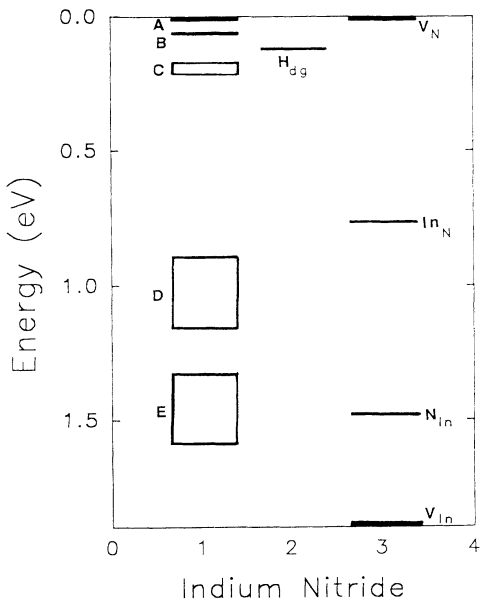

FIG. 6. Distribution of defect levels in the band gap of InN. The states in column 1 are those reported from experimental studies and fall into five groups, A–E. Column 2 shows the result of donor-level calculations in the modified-hydrogenic approximation from Table I. Column 3 data are the electron states for the point defects indicated, as calculated in Ref. 26.

tween 7×10^{16} cm^{-3} and 10^{17} cm^{-3} at room temperature.[36] This group of samples reached an exhaustion region below 150 K with n in the range $(2.5-7)\times10^{16}$ cm^{-3}. No further variation in concentration was observed down to 25 K, a temperature at which $kT\approx2$ meV, the absence of carrier freeze out implying an additional donorlike level very close to, or resonant with, the band edge.

An important feature in the absorption spectrum of InN is a broad band centered at about 0.2 eV, and with a full width at half maximum (FWHM) of about 0.25 eV,[36] which has been interpreted as either a deeper donor level or a compensating acceptor.[26,27,36] The width of this peak precludes detailed analysis as a strictly hydrogenic state while its shallowness suggests that a deep-level approach is equally inappropriate, we therefore examine its properties in terms of a quantum-defect state in accordance with Eq. (5). Excitation thresholds are obtained by plotting the quantity $\alpha^{2/3}(\hbar\omega)^2$ versus $\hbar\omega$ as shown for three samples in Fig. 7. The plots show good linearity over an energy range of about 0.1 eV in each, with excitation thresholds of 0.155, 0.215, and 0.255 eV in samples of room-temperature electron concentration 5×10^{16}, 1×10^{18}, and 1×10^{19} cm^{-3}, respectively. The energies of peak absorption, corresponding to a normalized absorption of 1.0 in the figure, are 0.31, 0.37, and 0.41 eV, respectively. Threshold and peak energies both increase with electron concentration at a rate compatible with the filling of conduction-band states, as shown in Fig. 8. Here we have included both calculated Moss-Burstein shift and the smaller shift observed experimentally in apparent band-gap changes which include an empirical component of band tailing.[1] The shift in absorption edge is intermediate between these two and indicates a low-concentration limit of about 0.15 eV for the threshold energy. Also evident is the predicted relationship between

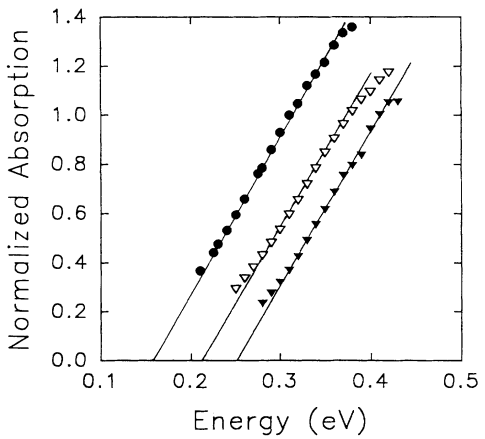

FIG. 7. Analysis of absorption data in the broad band at about 0.2 eV in InN for three different electron concentrations: $n\approx5\times10^{16}$ cm^{-3} (●), $n\approx10^{18}$ cm^{-3} (▽), and $n\approx10^{19}$ cm^{-3} (▼). In accordance with expected quantum-defect behavior, absorption coefficient α is plotted as the "normalized absorption" function $\alpha^{2/3}/(\hbar\omega)^{1/2}$ against photon energy ($\hbar\omega$). Each plot has been scaled to unity at the energy of the absorption peak.

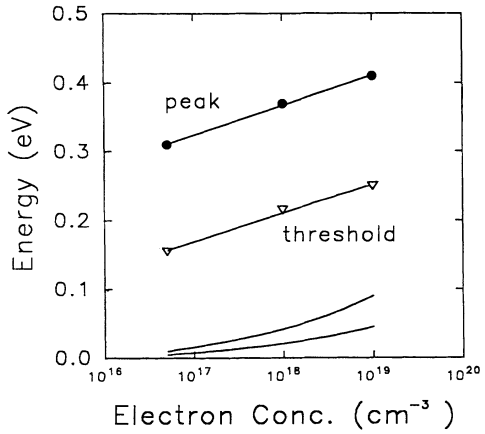

FIG. 8. Electron concentration dependence of peak (●) and threshold (▽) energies in the 0.2-eV InN band extracted from Fig. 6. Also shown are the observed Moss-Burstrein shifts for band-to-band absorption from Ref. 36 (lower curve), and the calculated shift with band tailing neglected (upper curve).

peak and threshold energies, the ratio being close to 2 in the low-concentration limit and falling to 1.6 at high levels. Evidence thus points to a relatively deep donor level at about 150 meV below the conduction band with a second level at 40 meV. The energy of the former is close to the predicted hydrogenic ground state for the double donor associated with the nitrogen vacancy and within the range predicted by deep-level calculations.[26] Details of its absorption line shape are better described, however, by a quantum-defect analysis intermediate between these two approaches. The shallower level becomes identifiable as elevated by Coulomb interaction when the donor is doubly occupied.

The persistence of a signification electron concentration down to temperatures where kT is of the order of 2 meV indicates that the prediction[26] of a third donor level, resonant with the conduction band, is also correct. Finally we note that absorption strength within this band increases with electron, and therefore donor concentration[36] as the above interpretation would require.

2. *Deep levels*

When free carriers are excited in n-type InN, charge balance requires $n\approx N_D^+$. However, mobility measurements indicate that ionized impurity scattering involves a component due to charged, compensating acceptors. Compensation ratios N_D^+/N_A^- between about 1.3 and 3 have been inferred.[7] This evidence suggests the involvement of the $\mathrm{In_N}$, V_{In}, and $\mathrm{N_{In}}$ defects, each of which includes hole states which would be empty (of holes) and therefore carry a negative charge when the Fermi level lies close to the conduction-band edge. Two absorption features, appearing as longer wavelength tails on the band-to-band absorption edge, can be identified as follows.

In low-doped material, $n<2\times10^{17}$ cm^{-3}, plots of α^2 versus $\hbar\omega$ yield straight lines[36] with thresholds E_{DP} between 0.9 and 1.2 eV in accordance with the prediction

for $|p\rangle$-like states of Eq. (6b). The apparent threshold energy varies strongly with electron concentration for this group of samples with the shallowest (0.9 eV) occurring in $n = 2.3 \times 10^{17}$ cm^{-3} material and the deepest (1.2 eV) in our lightest doped sample at $n = 1.1 \times 10^{17}$ cm^{-3}.

In higher-doped samples, $n > 5 \times 10^{17}$ cm^{-3}, an absorption tail with threshold energies between 1.35 and 1.65 eV, and no systematic variation with electron concentration, is observed. This result is obtained from linear plots of $\alpha^{2/3}(\hbar\omega)$ versus $\hbar\omega$, an example with $E_{DS} = 1.5$ eV is shown in Fig. 4 and indicates the involvement of $|s\rangle$-like states as shown by Eq. 6(a).

These two defect bands may be associated with the calculated[26] In_N levels at about 0.8 eV and deeper N_{In} levels at about 1.5 eV. We note, however, that low electron concentrations are obtained experimentally by increasing nitrogen content in order to minimize V_N donor concentrations, at the same time increasing N_{In}. Similarly, reduced nitrogen concentration yields higher electron concentrations brought about by the increase in V_N while commensurate with this would be an increase in M_N. The experimental 1-eV level in low-doped material is therefore more plausibly associated with the presence of N_{In} while the deeper 1.5-eV level can be associated with its converse In_N.

C. Aluminum nitride

A surprising volume of information is available on AlN although its popularity stems from its use in coatings rather than its semiconducting properties. Thus while it is relatively simple to prepare, until recently material quality has not been optimized for electronic properties and the values available are many and varied. Those attracting some consensus are collected in Fig. 9, along with the modified hydrogenic result and the predictions of Jenkins and Dow. The experimental levels are broadened (when compared with those of InN and GaN) because of the vast number of reported values, some of which may represent less-than-electronic grade material.

Again the range of values reported for the donor excitation falls into three groups at about 170, 500, and 800–1000 meV.[12,52–55] Recently, we have reported a study of thermally activated conductivity in AlN,[22] identifying a deep donor level at 790 meV (Fig. 9). This agrees surprisingly well with the values predicted from the hydrogenic (800 meV) and deep-level (500 and 1000 meV) approaches in view of the shortcomings of each in this energy range. By analogy with InN and GaN it is therefore reasonable to assume that a donor triplet at about 200 meV, 500 meV, and 900 eV is associated with V_N in AlN.

A deeper level with threshold 1.4–1.85 eV (Refs. 18, 19, 54, 56, and 57) has been repeatedly observed and can be identified with the calculated level of 1.6 eV for N_{Al}.

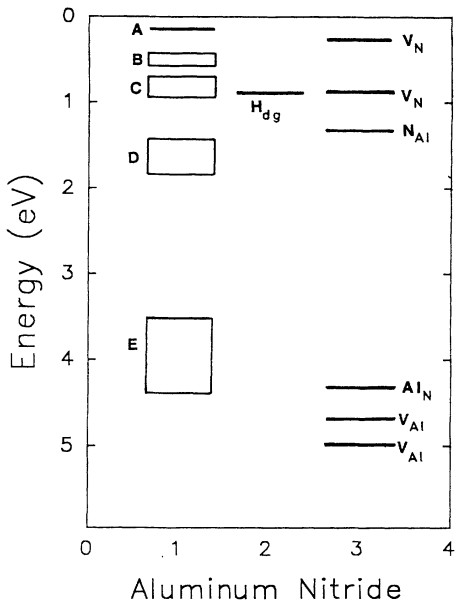

FIG. 9. Distribution of deep levels in the band gap of AlN. The states in column 1 are those reported from experimental studies and fall into five groups A–E. Column 2 shows the results of donor-level calculations in the modified-hydrogenic approximation from Table I. Column 3 data are the electron states for the point defects indicated, as calculated in Ref. 26.

Deep-level excitations have been observed with a range of thresholds. The band-tail absorption analyzed in the same way as for InN and GaN is included in Fig. 4 and has a range of thresholds between 3.4 and 4.5 eV. An example at 4.5 eV is shown, with other workers have reported 3.45,[33] 3.1–3.7,[56] and 4.2 eV.[57] Although the V_{Al} levels are predicted to lie within this range, the similarity of behavior to the metal antisite defects in InN and GaN suggest that Al_N is responsible.

IV. SUMMARY AND CONCLUSIONS

Median values of experimentally reported defect-related levels in the three group-III metal nitrides are brought together in Table II. A common feature is the presence of a triplet of shallow, donorlike levels associated with nitrogen vacancies the depth of which increases for lighter occupants of the metal site. The presence of deeper, compensating antisite defects becomes thermodynamically less probable[27] as the atomic mass difference between group-III and -V components increases. Thus InN, with very shallow and uncompensated donors is in-

TABLE II. Probable assignment of experimental data (median values).

Nitride	V_N, donor triplet (meV)			N_M (eV)	M_N (eV)	V_M (eV)	E_G (eV)
InN	0	40	150	1.05	1.5		1.89
GaN	30	110	390	0.9	2.3	3.264	3.4
AlN	170	500	900	1.7	4.5		5.9

variably an n-type semiconductor, while AlN, with a much deeper donor and high compensation levels, is invariably an insulator. GaN lies between these extremes of behavior, as might be expected from a combination of a donor of moderate depth and some tendency to compensation, and the selection of growth method dictates the conductivity obtainable. It is worth noting that the available level of control in as-grown GaN is commensurate with the much greater effort thus far devoted to it.

Because it is (a) heavily occupied and (b) sufficiently shallow to have a large optical cross section for excitation to the conduction band, the 150-meV donor level in InN provides a signification spectral absorption feature. Examination of this level in quantum-defect terms is fruitful and revised threshold values[1] are obtained. Threshold energy varies with electron concentration in the conduction band in a way entirely compatible with the band-filling process responsible for the Moss-Burstein shift[36] in optical band gap. A low-electron-concentration limit of 150 meV is deduced.

A hydrogenic treatment of donor levels yields results close to those obtained experimentally, surprisingly since both depth and complexity would suggest the approach to be inappropriate.

Deep levels in gallium and aluminum nitrides, in most respects, appear to have the general features predicted by Jenkins and Dow. The location of the N_{Al} antisite defect at about 1.7 eV is well substantiated by a number of reports in the range 1.4–1.8 eV while the N_{Ga} prediction of about 0.45 eV is somewhat shallower than experimental data between 0.8 and 0.9 eV. The M_N antisite and V_M vacancy defects all lie within the bottom half of the respective bands and are manifest as absorption tails on direct band-to-band spectral edges. Here additional information on the $|s\rangle$- or $|p\rangle$-like character of the defect helps in identification.

The only point defect unambiguously located appears to be the gallium vacancy observed in studies of GaN luminescence at 3.26 eV below the conduction band and close to the calculated value of about 3.3 eV. The GaN band tail, and $|s\rangle$-like absorption feature with threshold in the 2.2–2.5-eV range, can therefore be attributed to the Ga_N antisite defect with some confidence. Similar $|s\rangle$-like features appear in AlN between 3.4 and 4.5 eV, a range embracing the predicted V_{Al} antisite defect, while its converse, Al_N, is calculated to lie somewhat deeper at about 5.2 eV. Studies of the effect on optical properties of the in-diffusion of excess aluminum strongly suggest that the $|s\rangle$-like feature is associated with Al_N rather than V_{Al}, a view supported by its similarity to GaN.

The situation in InN is less clearly related to the predicted levels for In_N at 0.8 eV and N_{In} at 1.5 eV. We find, in a large number of reactively sputtered samples which we will call type I, an $|s\rangle$-like level between 1.35 and 1.65 eV, experimentally similar to the M_N antisite defect in both gallium and aluminum nitrides and also at about $\frac{2}{3}$ band gap. Present in other samples is a type-II feature, rather shallower at 0.9–1.2 eV and of $|p\rangle$-like character which, if the above allocation is correct, is associated with N_{In}. These allocations are the reverse of the theoretical prediction.[26] Whether a sample is of type I or II depends upon the circumstances of its growth. Type I are typically prepared at higher growth rates and lower nitrogen pressure from less-nitrided targets, conditions which yield high nitrogen vacancy concentrations evident in high electron densities ($n > 5\times10^{17}$ cm^{-3}), and more favorable to the generation of In_N antisite defects. Type II, on the other hand, are grown at lower rates, with higher nitrogen pressures and from fully nitrided targets. These conditions yield low V_N concentrations ($n < 2\times10^{17}$ cm^{-3}) and are conducive to N_{In} antisite formation. Accordingly we conclude that the levels associated with nitrogen occupancy of indium sites is shallower, at about 1 eV, than its converse at about 1.5 eV.

It may be observed that, for the predictions of Jenkins and Dow,[26] a reversal in the order of M_N and N_M levels occurs with increasing mass or atomic radius of the metal. The theory of Hjalmarson *et al.*[31] determines defect level energies from a Koster-Slater model, considering next-nearest-neighbor matrix elements only, where the defect potential is taken to be proportional to the difference in atomic orbital energies. It may be suggested, from the experimental data, that the theory predicts a reversal of the ordering of the levels, as a function of atomic mass, too early in the case of the nitrides.

ACKNOWLEDGMENTS

This work was supported by the Australian Research Council (ARC) and the Australia Telecommunications Research Board (ATERB).

[1]T. L. Tansely and C. P. Foley, J. Appl. Phys. **59**, 3241 (1986).
[2]H. J. Hovel and J. J. Cuomo, Appl. Phys. Lett. **20**, 71 (1972).
[3]J. W. Trainor and K. Rose, J. Electron. Mater. **3**, 821 (1974).
[4]N Puychechevrier and M. Menoret, Thin Solid Films **36**, 141 (1976).
[5]H. Takeda and T. Hada, Toyama Kogyou Kute Semmon Gakko Kiyo **11**, 73 (1977).
[6]V. A. Tyagai, A. M. Evstigneev, A. N. Krasiko, A. F. Andreeva, and V. Ya. Malakhov, Fiz. Tekh. Poluprovodn. **11**, 2142 (1977) [Sov. Phys.—Semicond. **11**, 1257 (1977)].
[7]T. L. Tansely and C. P. Foley, Electron. Lett. **20**, 1066 (1984).
[8]H. G. Grimeiss, R. Groth, and J. Maak, Z. Naturforsch., Teil A **15**, 799 (1960).
[9]H. G. Grimeiss and B. Monemar, J. Appl. Phys. **41**, 4054 (1970).
[10]J. I. Pankove, E. A. Miller, and J. E. Berkeyheiser, RCA Rev. **32**, 383 (1971).
[11]R. Dingle, K. L. Shaklee, R. F. Leheny, and R. B. Zetterstrom, Appl. Phys. Lett. **19**, 5 (1971).
[12]M. Ilegems, R. Dingle, and R. A. Logan, J. Appl. Phys. **43**, 3797 (1972).
[13]R. D. Cunningham, R. W. Brander, N. D. Knee, and D. K. Wickenden, J. Lumin. **5**, 21 (1972).
[14]H. Amano, N. Sawaki, I. Akasaki, and Y. Toyoda, Appl. Phys. Lett. **48**, 353 (1986).
[15]K. Naniwae, S. Itoh, H. Amano, K. Itoh, K. Hiramatsu, and

I. Akasaki, J. Cryst. Growth **99**, 381 (1990).
[16]B. Monemar, O. Lagerstedt, and H. P. Gislason, J. Appl. Phys. **51**, 625 (1980).
[17]R. Madar, G. Jacob, J. Hallais, and R. Fruchart, J. Cryst. Growth **31**, 197 (1975).
[18]Hiroshi Amano, Masahiro Kito, Kazumasa Hiramutsu, and Isamu Akasaki, Jpn. J. Appl. Phys. **28**, 2112 (1989).
[19]G. A. Cox, D. O. Cummins, K. Kawabe, and R. H. Tredgold, J. Phys. Chem. Solids **28**, 543 (1968).
[20]H. Demiryont, L. R. Thompson, and G. J. Collins, J. Appl. Phys. **59**, 3235 (1986).
[21]Li Xinjiao, Xu Zechnan, He Zujou, Cao Huazhe, Su Wuda, Chen Zhongcai, Zon Feng, and Wang Erguang, Thin Solid Films **139**, 261 (1986).
[22]Xin Li and T. L. Tansely, J. Appl. Phys. **68**, 5369 (1990).
[23]M. Mizuta, S. Fujieda, T. Jitsukawa, and Y. Matsumoto, in Proceedings of the 13th International Symposium on GaAs and Related Compounds, edited by W. T. Lindley, IOP Conf. Proc. No. 83 (Institue of Physics and Physical Society, London, 1986), p. 153.
[24]K. Akimoto, I. Hirosawa, J. Mizuki, S. Fujieda, Y. Matsumoto, and J. Matsui, Jpn. J. Appl. Phys. **27**, L1401 (1988).
[25]Y. Mochizuki, M. Mizuta, S. Fumieda, and Y. Matsumoto, Appl. Phys. Lett. **55**, 1318 (1989).
[26]David W. Jenkins and John D. Dow, Phys. Rev. B **39**, 3317 (1989).
[27]T. L. Tansley, R. J. Egan, and E. C. Horrigan, Thin Solid Films **164**, 441 (1988).
[28]B. K. Ridley, *Quantum Processes in Semiconductors*, 2nd ed. (Clarendon, Oxford, 1988).
[29]W. Y. Hsu, J. D. Dow, D. J. Wolford, and B. G. Streetman, Phys. Rev. B **16**, 1597 (1977).
[30]W. A. Harrison, *Electronic Structure and the Properties of Solids* (Freeman, San Francisco, 1980).
[31]H. P. Hjalmarson, P. Vogl, D. J. Wolford, and J. D. Dow, Phys. Rev. Lett. **44**, 810 (1980).
[32]C. P. Foley andJ. Lyngdal, J. Vac. Sci. Technol. A **5**, 1708 (1987).
[33]J. Pastrnak and L. Roskovcova, Phys. Status Solidi **26**, 591 (1968).
[34]F. S. Ohuchi and R. H. French, J. Vac. Sci. Technol. A **6**, 1695 (1988).
[35]T. L. Tansley and C. P. Foley, in *Proceedings of the Third International Conference on Semi-Insulating III-V Materials, Warm Springs, Oregon, 1984,* edited by J. Blakemore (Shiva, London, 1985), pp. 497–500.
[36]T. L. Tansley and C. P. Foley, J. Appl. Phys. **60**, 2092 (1986).
[37]R. Dingle, D. D. Sell, S. E. Stokovski, and M. Ilegems, Phys. Rev. B **4**, 1211 (1971).
[38]J. I. Pankove, S. Bloom, and G. Harbeke, RCA Rev. **36**, 163 (1975).
[39]R. Dingle and M. Ilegems, Solid State Commun. **9**, 175 (1971).
[40]B. Monemar and O. Lagerstedt, J. Appl. Phys. **50**, 6480 (1979).
[41]J. C. Veseley, M. Shatzkes, and P. J. Burkhardt, Phys. Rev. B **10**, 582 (1974).
[42]V. S. Vavilov, S. I. Makarov, M. V. Chukichev, and I. V. Chetverikova, Fiz. Tekh. Poluprovodn. **13**, 2153 (1979) [Sov. Phys.—Semicond. **13**, 2153 (1979)].
[43]J. I. Pankove, H. P. Maruska, and J. E. Berkeyheiser, Appl. Phys Lett. **17**, 197 (1970).
[44]M. Ilegems and R. Dingle, J. Appl. Phys. **44**, 4234 (1973).
[45]O. Lagerstedt and B. Monemar, J. Appl. Phys. **45**, 2266 (1974).
[46]B. Monemar, Phys. Rev. B **10**, 676 (1974).
[47]J. I. Pankove, J. E. Berkeyheiser, and E. A. Miller, J. Appl. Phys. **45**, 1280 (1974).
[48]Toshio Ogino and Masahuri Aoki, Jpn. J. Appl. Phys. **18**, 1049 (1979).
[49]J. I. Pankove, M. T. Duffy, E. A. Miller, and J. E. Berkeyheiser, J. Lumin. **8**, 89 (1973).
[50]Toshio Ogino and Masahuri Aoki, Jpn. J. Appl. Phys. **19**, 2395 (1980).
[51]J. I. Pankove and J. A. Hutchby, J. Appl. Phys. **47**, 5387 (1976).
[52]J. Edwards, K. Kawabe, G. Stevens, and R. H. Tredgold, Solid State Commun. **3**, 99 (1965).
[53]Mizuho Morita, Kazuo Tsubouchi, and Nobou Mikoshiba, Jpn. J. Appl. Phys. **21**, 728 (1982).
[54]Akiko Kobayashi, Otto F. Sankey, and John D. Dow, Phys. Rev. B **28**, 946 (1983).
[55]M. Gautier, J. P. Duraud, and C. Le Gressus, Surf. Sci. **178**, 201 (1986).
[56]Jean Lagrenaudie, J. Chim. Phys. **53**, 222 (1956).
[57]R. W. Francis and W. L. Worrell, J. Electrochem. Soc. **123**, 430 (1976).